

# Charge Inversion of a Macroion in Spherical and Rod Shapes for Different Coions and Polymer Counterions: Electrophoresis by Molecular Dynamics Simulations

Motohiko Tanaka

*National Institute for Fusion Science, Toki 509-5292, Japan*

(Dated: March 24, 2003)

By molecular dynamics simulations we show the effects of coion radius and valence, polymer counterions and monovalent salt on the electrophoretic mobility of a macroion in spherical and rod shapes. The reversed mobility increases with the ratio of coion to counterion radii  $a^-/a^+$ , which peaks at an intermediate value of  $a^-/a^+$ . It decreases with the ratio of coion to counterion valences  $Z^-/Z^+$ , and becomes non-reversed for  $Z^-/Z^+ > 1$ . The monovalent salt suppresses reversed mobility, except for mobility enhancement of a strongly charged macroion at small salt ionic strength. There is a threshold surface charge density for charge inversion to take place. Polymers (polyelectrolyte) consisting of multivalent counterions are favorable for charge inversion of a weakly charged rod macroion like DNA. The reversed mobility of an elongated macroion can be enhanced by mechanical twining of polyelectrolyte counterions around the rod axis.

PACS numbers: 61.25.Hq, 82.45.-h, 82.20.Wt

## I. INTRODUCTION

The phenomenon of reverting the charge sign of large ions due to other ions and salts in water solution was known to physical chemists as charge inversion or over-screening for half a century [1]. More recently, it also attracted a significant attention of physicists [2, 3, 4, 5, 6, 7, 8, 9]. It is now understood that charge inversion is the generic phenomenon that occurs in strongly correlated charged systems. It has far reaching consequences in biological and chemical worlds. In particular, it seems to be a decisive ingredient in modern gene therapy, facilitating the uptake of genes (negatively charged DNA) by predominantly negative cell walls [10].

In our previous papers [6, 7], we worked out a molecular dynamics model adequate to examine charge inversion. More specifically, we studied the electrophoretic mobility problem [7], and showed that a charge inverted complex drifts under the external electric field in the direction determined by its inverted charge. The net charge of the macroion complex was deduced by the force balance,  $Q^* \sim \nu\mu$ , where  $\mu$  is the electrophoretic mobility and  $\nu$  is the solvent friction enhanced by Debye screening of hydrodynamic interactions [11].

The goal of this paper is to extend our studies by addressing three new aspects of charge inversion: dependences on the coion properties, the role of monovalent salt, and charge inversion of a weakly charged rod-shaped macroion like DNA [12]. Previously we assumed that both counterions and coions are spheres of the same radius. But, anions usually have larger radii than cations for monovalent salt including NaCl. We also assumed that coions were all monovalent while counterions were multiply charged, which is the necessary condition for charge inversion. Here, we relax these assumptions and examine first the effects of radius and valence of coions on the electrophoretic mobility of a macroion immersed in a solution of the  $Z^+ : Z^-$  multivalent salt. We look at the cases of some experimental environments with mono-

valent salt that exists as the base of the  $Z : 1$  salt. Furthermore, we study the cases of an elongated rod-shaped macroion in the presence of spherical or polymer counterions (polyelectrolyte).

We take the system of a macroion, coions/counterions and neutral particles, and solve the Newton equations of motion with the Coulombic and Lennard-Jones potential forces under an applied electric field  $E$  ( $E > 0$ ). We adopt the repulsive Lennard-Jones potential,  $\phi_{LJ} = 4\varepsilon[(\sigma/r_{ij})^{12} - (\sigma/r_{ij})^6]$  for  $r_{ij} = |\mathbf{r}_i - \mathbf{r}_j| \leq 2^{1/6}\sigma$ , and  $\phi_{LJ} = -\varepsilon$  otherwise, except some runs in Sec.IV. Here  $\mathbf{r}_i$  is the position vector of the  $i$ -th particle, and  $\sigma$  is the sum of the radii of two interacting particles, which are chosen as follows: radius of the macroion  $R_0$ , the radii of counterions and coions  $a^+$  and  $a^-$ , respectively, with  $a^+ = a$  fixed, and neutral particles  $a/2$ , where  $a$  is the unit of length. We relate  $\varepsilon$  with the temperature by  $\varepsilon = k_B T$ . The Bjerrum length is  $\lambda_B = e^2/\epsilon k_B T$  where  $\epsilon$  is dielectric constant of the solvent. We adopt neutral particles to model the viscous solvent of given temperature and to treat the interactions among the finite-size macroion, counterions, coions and the solvent. Since the hydrodynamic interactions in the electrolyte solvent are screened at short distances comparable to the Debye length [7, 11], the use of thermal bath to drain the Joule heat is not affecting our results. For the details of the employed model and molecular dynamics method, we refer the readers to our previous work [7].

We use the following parameters in this paper unless otherwise specified. The simulation system is a three-dimensional periodic box of the side  $L = 32a$ . Our choice of the temperature (the ratio of electrostatic energy to thermal energy) is  $e^2/\epsilon a k_B T = 5$ , which implies  $a \cong 1.4\text{\AA}$  in water. We set the macroion radius  $R_0 = 5a$ , charge  $Q_0 \sim -80e$ , and mass  $200m$ . The mass of counterions and coions is  $m$ , where  $m$  is the unit of mass. Each neutral particle has mass  $m/2$  and occupies approximately a volume element  $(2.1a)^3 \cong (3\text{\AA})^3$ , except for the volume already occupied by other ions. The external electric field

is  $E = 0.3\epsilon/ae$ .

In Sec.II we examine the effects of coion radius and valence on charge inversion. Next in Sec.III, we study the effects of monovalent salt. We introduce a rod-shaped macroion that can adsorb more counterions than a spherical one for the same surface charge density, which lowers the charge inversion threshold. Following these results, we adopt in Sec.IV a macroion with double helix charge distribution and polymer cations, as in the experiments of charge inversion for DNA. Sec.V will be a brief summary of the present paper.

## II. THE EFFECTS OF COION PROPERTIES

The dependence of electrophoretic mobility on the radius of coions for the fixed counterion radius,  $a^+ = a$ , is shown in Fig.1. The macroion has charge  $Q_0 = -80e$ , and radius  $R_0 = 5a$ ; the valence of counterions is  $Z^+ = 3$  (open circles), 5 (filled circles), and 7 (triangles); coions are monovalent and their number is  $N^- \sim 60$ . The number of counterions is determined from charge neutrality.

In the figure the mobility is reversed (positive) and increases with the ratio of coion to counterion radii up to  $a^-/a^+ \approx 1.5$ , irrespectively of the counterion valences. This increase is due to geometrical difficulties for two coions to condense on one counterion by avoiding each other if their radius is large. This leads to reduced charge neutralization of the macroion complex. The increase with the radius ratio of two ion species is in line with a previous study of the finite coion size effect for charge inversion [3], and also with condensation of the  $Z : 1$  electrolyte ions that have size asymmetry [13]. Interestingly, the mobility is extrapolated to the origin when the coion radius is very small in comparison with that of counterions, implying good charge shielding by charge cloud like in high-temperature electrolyte liquid and plasmas.

For large radius ratio  $a^-/a^+ \geq 1.5$ , the mobility turns into decrease. This is also the case for the weak external field  $E = 0.1\epsilon/ae$ , thus eliminating the possibility of collisional effect between ions. Instead, this decrease is attributed to the less degree of coion contributions to the charge inversion process. The radial distribution functions tell us that the coions with large radius are more separated from the counterions adsorbed on the macroion, and that the number of such counterions becomes largest at  $a^-/a^+ \approx 1.5$ . We showed in our previous paper [6] that large charge inversion requires both counterions and coions. Namely, the coions need to be properly redistributed to minimize the system energy while confining some counterions to the very vicinity of the macroion. With large coions this mechanism does not work, and the number of the counterions near the macroion needs to be reduced by charge neutrality.

The effect of coion valence  $Z^-$  on electrophoretic mobility is shown in Fig.2 for fixed counterion valences  $Z^+$ . The counterions are either trivalent or tetravalent, the macroion charge and radius are  $Q_0 \sim -80e$  and  $R_0 = 5a$ , respectively. The number of the coions is

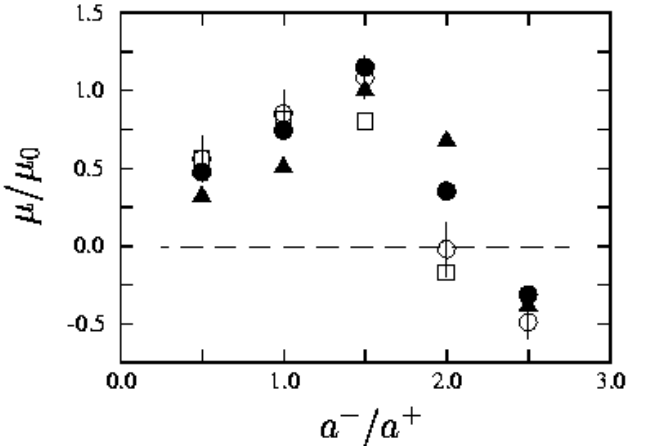


FIG. 1: The dependence of macroion mobility  $\mu$  on the coion radius against the ratio of coion to counterion radii  $a^-/a^+$ , where  $\mu_0 = v_0/(|Q_0|/R_0^2)$  with  $v_0$  being the thermal velocity of neutral particles. The charge and radius of the macroion are  $Q_0 \sim -80e$  and  $R_0 = 5a$ , respectively, the valence of counterions is  $Z^+ = 3$  (open circles), 5 (filled circles), and 7 (triangles). The external field is  $E = 0.3\epsilon/ae$  for above cases, and  $E = 0.1\epsilon/ae$  for  $Z^+ = 3$  (squares). The temperature is  $e^2/\epsilon a k_B T = 5$ . The number of monovalent coions is approximately  $N^- \sim 60$ .

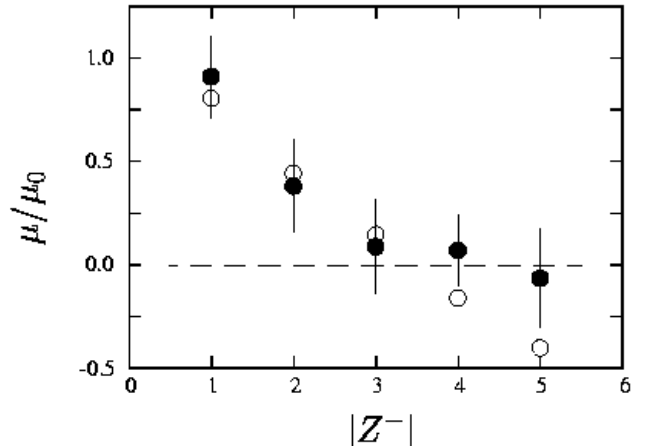


FIG. 2: The dependence of the macroion mobility against the coion valence  $Z^-$  for fixed counterion valences  $Z^+ = 3$  (open circles) and  $Z^+ = 4$  (solid circles). The radii of coions and counterions are equal,  $a^-/a^+ = 1$ . The external electric field is  $E = 0.3\epsilon/ae$ , and the temperature is  $e^2/\epsilon a k_B T = 5$ .

$N^- = 300/|Z^-|$ , and that of the counterions is determined by charge neutrality condition. The coions and counterions have equal radii,  $a^-/a^+ = 1$ . For the monovalent coions, the mobility is reversed and largest. As the coion valence increases, the magnitude of reversed mobility decreases linearly until the two valences become equal  $Z^+ \sim |Z^-|$ . The mobility is small but positive for the equal valences, above which the mobility turns to negative (non-reversed). This result is similar to that of Fig.1

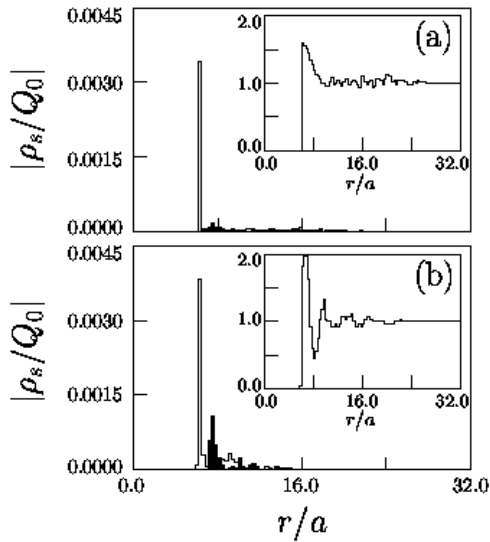


FIG. 3: The radial distribution functions of charge density  $\rho_s$  of counterions (solid) and coions (shaded) for the coion valence (a)  $Z^- = -1$  and (b)  $Z^- = -3$  for the runs in Fig.2. The counterion valence is  $Z^+ = 3$ . The inset panels show the integrated charge distribution  $Q(r)/|Q_0|$  of the corresponding charge densities of counterions and coions.

in terms of charge neutralization efficiency by coions.

It is also noted that the result of Fig.2 is in line with the theory of the HNC-MSA integral equations [8] which reported reversed mobility for the case of divalent counterions and coions,  $Z^+ = |Z^-| = 2$ . The case of  $Z^+ = |Z^-|$  is close to the situation of the normal Debye screening, except for the unusually low temperature. We note that, when temperature is low, the Debye theory is not applicable and one should instead use nonlinear Poisson-Boltzmann theory which does not provide for charge inversion. However, when there are strongly charged ions of finite radii and both signs, there occur strong correlations where even the nonlinear Poisson-Boltzmann theory fails to result in charge inversion.

Indeed, we observe strong correlations of *multivalent* coions with counterions in the radial distribution function of charge density of Fig.3. The panel Fig.3(b) for  $|Z^-| = 3$  shows enhanced association of multivalent coions with the surface counterions. The positive macroion complex is surrounded by a sharp negatively charged layer, which distinctly separates the macroion complex from the rest of the ion atmosphere. The integrated charge distribution  $Q(r) = \int \sum_s \rho_s(r') d^3 r'$  in the inset panel of Fig.3(b) better illustrates this situation, where the integration starts at the macroion surface  $r = R_0$  and the summation goes over counterions and coions. The width of the positively charged layer becomes as small as  $1.3a$  for  $Z^- = -3$ , whereas it is  $3.4a$  for  $Z^- = -1$  in Fig.3(a). Each multivalent coion thus firmly condenses to the counterion in the former case and efficiently reduces the positive charges of the macroion complex.

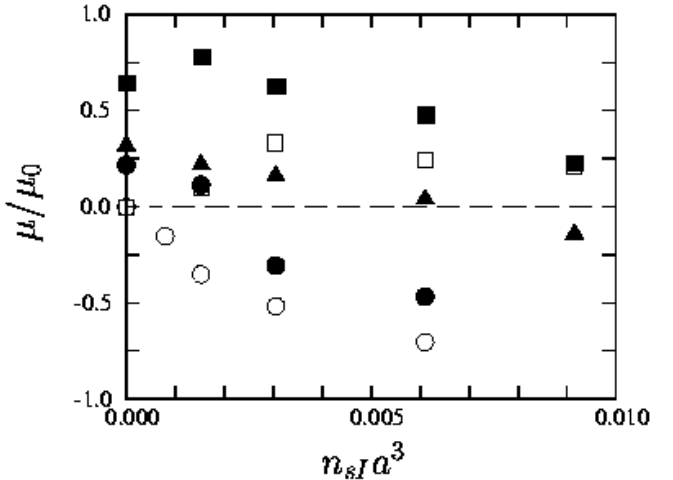


FIG. 4: The mobility of the spherical and rod-shaped macroions is shown against ionic strength of monovalent salt  $n_{si} = 2N^{+1}/L^3$ , where  $N^{+1}$  is the number of monovalent counterions. Squares and circles correspond to the spherical macroion, and triangles to the rod macroion. The parameters at zero salt  $n_{si} = 0$  for the spherical macroion with  $R_0 = 5a$  are:  $Q_0 = -81e$ ,  $N^{+3} = 37$ ,  $N^- = 30$  (filled squares),  $Q_0 = -81e$ ,  $N^{+3} = 27$ ,  $N^- = 0$  (no excess Z- ions, open squares),  $Q_0 = -21e$ ,  $N^{+3} = 17$ ,  $N^- = 30$  (filled circles), and  $Q_0 = -21e$ ,  $N^{+3} = 7$ ,  $N^- = 0$  (open circles). For the rod macroion,  $Q_{rod} = -100e$ ,  $R_{rod} = 5a$ ,  $L_z = 32a$ ,  $N^{+3} = 64$ ,  $N^- = 92$  (filled triangles).

### III. THE EFFECTS OF MONOVALENT SALT AND ROD-SHAPED MACROION

Now we study the effects of monovalent salt that exists as the base component to the multivalent salt. We treat the cases of both a spherical macroion and a rod-shaped macroion placed in the solution of Z:1 and 1:1 salt of spherical ions. The common parameters in this section are the trivalent counterions  $Z = 3$ , and the equal radii for coions and counterions  $a^- = a^+ = a$ .

Figure 4 shows the dependence of mobility against the ionic strength of monovalent salt,  $n_{si} = 2N^{+1}/L^3$ , where  $N^{+1}$  is the number of monovalent counterions which is equal to that of matching monovalent coions. The salt ionic strength at  $N^{+1} = 50$  is  $n_{si} \sim 0.0031/a^3$ . Here, the normalization  $\mu_0 = v_0 R_{00}^2 / |Q_{00}|$  is used for both the spherical and rod-shaped macroions, where  $Q_{00} = -81e$  and  $R_{00} = 5a$ .

It is interesting that addition of small amount of monovalent salt enhances the reversed mobility for a strongly charged macroion of the spherical shape (filled squares) whose surface charge density is  $\sigma_{sp} = Q_0 / 4\pi R_0^2 \sim 0.25e/a^2$ . Even for the case without excess Z-ions for which  $N^{+3} = |Q_0|/eZ$  (open squares), charge inversion is induced by addition of monovalent salt. This is attributed to monovalent counterions with small Wigner-Seitz cell radius  $R_W = 2R_0(eZ/|Q_0|)^{1/2} \sim 1.1a$  compared to multivalent ones. Namely, the monovalent coun-

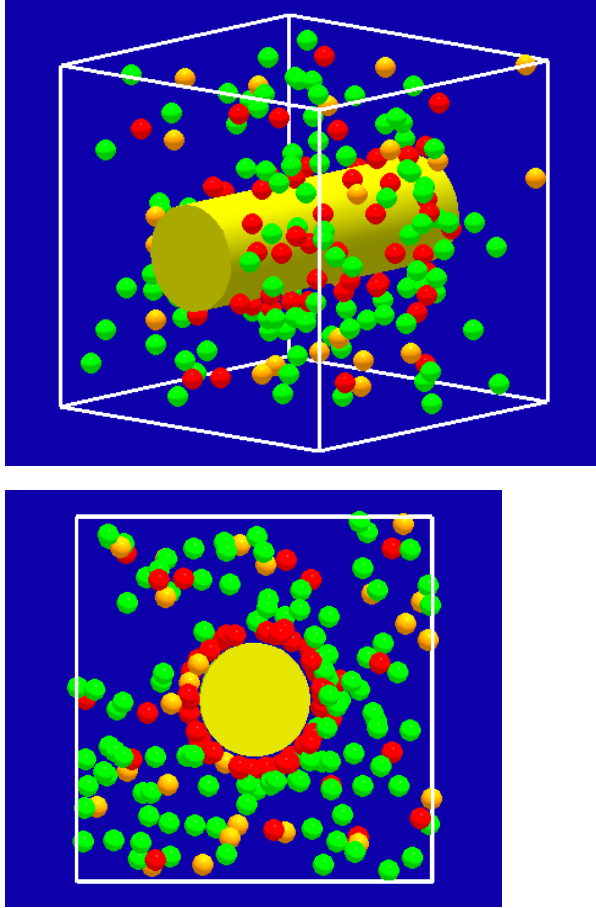


FIG. 5: The bird's-eye view (top) and the side view (bottom) of all the ions for the rod macroion with  $Q_{rod} = -100e$  at ionic strength  $n_{sI} \sim 0.0015/a^3$  in Fig.4. The small ions are trivalent counterions  $N^{+3} = 64$  (red), monovalent coions  $N^- = 117$  (green), and the monovalent positive salt  $N^+ = 25$  (yellow). (Neutral particles are not shown).

terions can optimally fill the regions that have not been occupied by Z-ions on the macroion surface, which thus increases the inverted charge of the macroion complex. The peak of the reversed mobility for the case with less Z-ions (more empty spaces to fill in) occurs at higher salt ionic strength, which is consistent with the above explanation. However, addition of large amount of monovalent salt simply shields the electric field and decreases the reversed mobility. By extrapolation, termination of reversed mobility is expected at  $n_{sI} \sim 0.013/a^3$  or  $N^{+1} \sim 200$  for this system.

The open and filled circles in Fig. 4 show the cases of a weakly charged macroion of the spherical shape with  $Q_0 = -21e$  for trivalent Z-ions with  $N^{+3} = 7$  and 17, respectively. The surface charge density is  $\sigma_{sp} = 0.067e/a^2$ . For the former, the number of the Z-ions is just sufficient to neutralize the macroion; charge inversion is not observed. For the latter case, ten extra Z-ions exist on top of  $|Q_0|/eZ = 7$  neutralizing ions. The mobility is re-

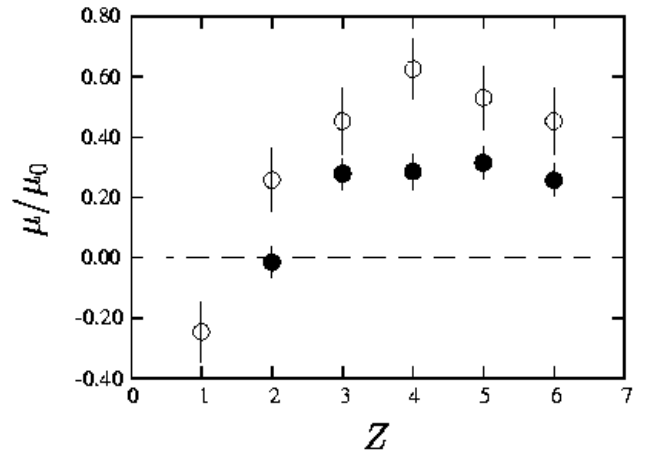


FIG. 6: Dependence of the mobility on the valence of the counterions  $Z$  for the rod-shaped macroion with radius  $R_{rod} = 5a$  and charge  $Q_{rod} = -100e$  (filled circles). The number of monovalent coions is fixed around  $N^- \sim 60$ . As reference, the case of the spherical macroion with  $R_0 = 5a$  and  $Q_0 = -80e$  [7] is shown by open circles.

versed at zero salt, and decreases monotonically with the salt ionic strength, which turns to normal (non-reversed) when the ionic strength of extra Z-ions is dominated by that of the monovalent salt.

We interpret that the rapid decrease in the mobility with salt ionic strength for the weakly charged macroion is due to the spherical shape of the macroion. Namely, a small number of Z-ions that can be adsorbed on the macroion are not sufficient to maintain electrostatic correlations while overcoming thermal fluctuations.

Thus, in the below we adopt a macroion of the rod shape, extending in full length to the  $z$  direction, with the radius  $R_{rod} = 5a$ . The surface charge density for  $Q_{rod} = -100e$  is  $\sigma_{rod} = Q_{rod}/2\pi R_{rod}L \sim 0.10e/a^2$  (filled triangles in Fig.4). The reversed mobility for the rod macroion is three times more persistent in terms of ionic strength of monovalent salt than for the spherical macroion with similar surface charge density.

The cases with large reversed mobility in Fig.4 are associated with the formation of Z-ion network on the surface of the macroion, irrespectively of spherical or rod shapes. Fig.5 shows the case of the rod macroion. As with the case of the strongly charged spherical macroion (cf. Fig.1 of [7]), majority (70%) of the Z-ions are adsorbed on the macroion surface, which is more than enough for charge neutrality requirement. By contrast, most of the monovalent counterions (80%) are detached from the macroion and homogeneously distributed. This is due to stronger binding forces on multivalent counterions to the macroion than for monovalent ones. Coions condense to the topside of the counterions on the macroion surface, and charge neutralization is completed in about  $3a$  from the surface.

Since we have learned that the shape (geometry) of

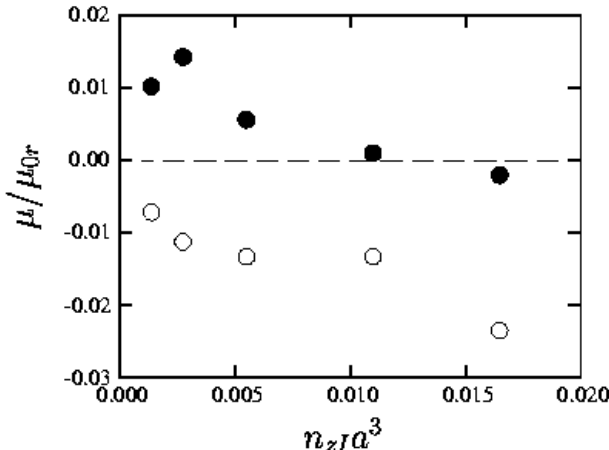


FIG. 7: The mobility of a rod macroion having double helix charge distribution against ionic strength of free counterions in the bulk. (a) Counterion polymers, each of which consists of three trivalent Z-ions (filled circles), and (b) all isolated trivalent counterions (open circles). The surface charge density of the macroion is roughly that of DNA,  $\sigma_{rod} \approx 0.02e/a^2$ , and the ratio of coion to Z-ion radii is  $a^-/a^+ = 1.5$ .

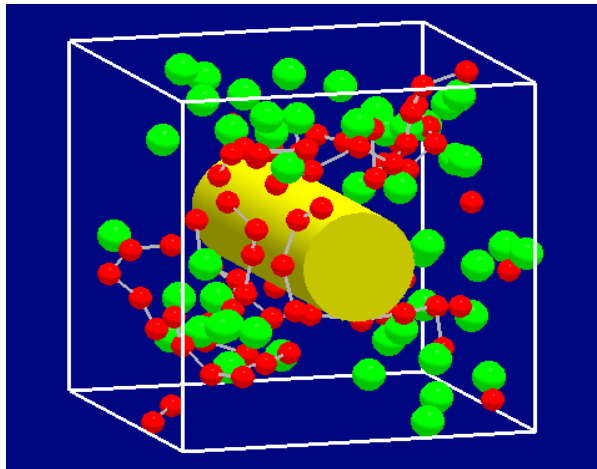


FIG. 8: The bird's-eye view of a weakly charged rod macroion with polyelectrolyte cations (red) and isolated anions (green). Double helix charges are aligned along the rod with  $Q_{rod} = -20e$ ,  $R_{rod} = 5a$  and  $L_z = 32a$  whose average charge density is approximately that of DNA. The polyelectrolytes made of four chains of connected 20 unit charges mechanically wind around the rod. The radius and number of anions are  $a^- = 1.5a$  and  $N^- = 60$ , respectively. (Neutral particles are not shown).

the macroion affects charge inversion, here we reexamine the effect of counterion valence on the electrophoretic mobility. Figure 6 shows the mobility against the valence  $Z$ . The surface charge densities are  $\sigma_{sp} = 0.26e/a^2$  for the spherical macroion and  $\sigma_{rod} = 0.10e/a^2$  for the rod macroion. Previously we showed that the mobility for the spherical macroion peaks around  $Z \approx 4$  (open circles)

[7], where the Wigner-Seitz cell radius  $R_W \sim 2.2a$  for  $Z = 4$  is comparable to the macroion radius  $R_0 = 5a$ . By contrast, the mobility for the rod macroion becomes reversed for  $Z > 2$  (filled circles) and then levels off due to the ease of the Z-ion network formation along the rod axis. Thus, the rod geometry even with a finite radius  $R_{rod} \sim 2R_W$  is already close to the plane geometry.

#### IV. A WEAKLY CHARGED MACROION: IS DNA SUBJECT TO CHARGE INVERSION ?

We show two cases of charge inversion for the weakly charged rod macroion whose average surface charge density is approximately that of DNA,  $\sigma_{rod} \approx 0.02e/a^2$ , as  $a \approx 1.4\text{\AA}$ . These cases include (i) double helix discrete charges lying at the depth  $a$  below the surface of a cylinder of radius  $R_{rod} = 5a$ , surrounded by polymer cations (polyelectrolyte) of Z-ions, and (ii) the above macroion and polymer cations of connected unit charges  $e$ . We keep the number of Z-ions above the neutrality requirement  $N^{+Z} > |Q_{rod}|/eZ$ . Counterions are trivalent  $Z = 3$ , and coions are monovalent with larger radius than counterions  $a^-/a^+ = 1.5$ , which is favorable for charge inversion (Sec.III). The temperature is  $e^2/\epsilon a k_B T = 5$ , and the external field is  $E = 0.1\epsilon/ae$ . In this section, the mobility normalization  $\mu_{0r} = v_0 R_{rod} L / 2|Q_{rod}|$  is used (about three times that of the value for the previous definition), which indexes to the surface electric field generated by the rod.

For the macroion having the double helix charge distribution, we obtain charge inversion for the polyelectrolyte cations of connected three Z-ions, as shown by filled circles in Fig.7. The reversed mobility increases with the Z-ion ionic strength and peaks at the ionic strength of free (not adsorbed) Z-ions  $n_zI \sim 0.0027/a^3$ . We note that ionic strength of the Z-ions to neutralize the macroion is  $0.0018/a^3$ . With further addition of Z-ions, the correlations between adsorbed and bulk Z-ions become significant, and the mobility decreases and becomes non-reversed for the ionic strength  $n_zI > 0.013/a^3$ . Here, the macroion is sterlic with the Lennard-Jones force being cut off at the distance  $r = 2^{1/6}a$ . Figure 7 also shows that charge inversion does not occur for the same macroion but when Z-ions are all isolated as denoted by open circles, or for a homogeneously charged macroion of the same surface charge density at any ionic strength of polyelectrolyte cations.

Two conclusions are drawn from the above simulation results. First, counterion polymers (polyelectrolytes) can cause charge inversion more efficiently than isolated counterions of the same ionic strength. Secondly, for a weakly charged macroion, localized surface charges are more advantageous than homogeneously distributed charges of the same surface charge density.

As the second case, we examine charge inversion due to polyelectrolyte cations consisting of unit charges. Short cation polymers with approximately less than ten unit

charges do not yield reversed mobility even at zero salt. For example, we get  $\mu \approx -0.10\mu_{0r}$  for the polyelectrolytes of connected three unit charges with their ionic strength  $\sim 5 \times 10^{-4}/a^3$ . Adsorption of such polyelectrolytes to the macroion is weak. The radial distribution function and the bird's-eye view plot tell us that a half of such polyelectrolytes are located away from the rod macroion, in clear contrast to the polyelectrolytes of connected three Z-ions in Fig.7. For polyelectrolyte of connected 20 unit charges, reversed mobility results  $\mu \approx 0.073\mu_{0r}$ . On the other hand, when the attraction part of the Lennard-Jones (LJ) potential  $k_B T$  is added without truncation at  $2^{1/6}\sigma$ , the reversed mobility is obtained for the polyelectrolyte of 10 unit charges,  $\mu \approx 0.015\mu_{0r}$ . This result is qualitatively similar to the theory predicting charge inversion (discrete surface charges) by polymer counterions of unit charges [14]. But, the molecular dynamics simulation requires more stringent circumstances for the occurrence of charge inversion.

The bird's-eye view of Fig.8 is a snapshot for the long counterion polymers of unit charges. Remarkably, we see mechanical twining of the polymer chains around the axis of a rod-shaped macroion. These chains are not statically adsorbed but repeat twining and untwining in time. Twining of counterion polymers which carry more charges than the macroion on time average pulls the rod macroion toward the electric field in the electrolyte solution. However, when the chain length is half and the number of the chains is doubled, we do not observe reversed mobility, for which the chains pass by the rod and the twining process is not effective enough to compensate the rod charge.

The mechanical twining of counterion polymers around the axis of a weakly charged macroion can enhance reversed electrophoretic mobility in reality. Although this is a different mechanism from that of electrostatic adsorption, it certainly helps to yield reversed mobility and the gene delivery based on electrophoresis.

## V. SUMMARY

In this paper, we focused on three aspects of charge inversion, namely, dependences on coion properties, the effectiveness of a rod macroion, and a weakly charged rod macroion corresponding to DNA.

First, we showed that a large coion radius played a positive role in charge inversion, while a large coion va-

lence did a negative role, both for fixed radius and valence of counterions. More specifically, the reversed mobility started at nearly null for very small coion radius, and increased with the ratio of the coion to counterion radii  $a^-/a^+$ . It peaked at the ratio  $a^-/a^+ \approx 1.5$ , and decreased for further increase in the ratio due to the reduction of coion correlations, since coions need to be involved for large charge inversion. On the other hand, the reversed mobility decreased with the ratio of the coion to counterion valences  $Z^-/Z^+$ , and charge inversion was terminated for the coion valence exceeding that of the counterions.

Secondly, monovalent salt shielded the electrostatic interactions and suppressed reversed mobility induced by the Z:1 salt, except that the monovalent salt at small ionic strength could enhance reversed mobility when a macroion is strongly charged. For a weakly charged macroion, this enhancement region was small and reversed mobility decreased monotonically and turned back to a non-reversed state.

Thirdly, there was a threshold of surface charge density for charge inversion to take place due to thermal fluctuations of adsorbed counterions. A rod-shaped macroion was more persistent to monovalent salt than a spherical macroion. The threshold corresponding to the DNA case was surpassed by a rod macroion of double-helix localized charges and cation polymers of multivalent counterions, with the help of large coions.

With the macroion in a rod shape, there occurred mechanical twining of cation polymers (polyelectrolyte) of unit charges around the axis of a weakly charged macroion. Combination of electrostatic adsorption and mechanical twining of polymer cations collaborated to reverse the sign of effective charges of the macroion complex. Thus, the macroion was subject to the electric drift under electrophoresis.

## Acknowledgments

The author is highly grateful to Prof.A.Yu.Grosberg for fruitful suggestions and discussions. He also thanks Prof.I.Ohmine for encouragements. The computation of the present study was performed with the Origin 3800 system of the University of Minnesota Supercomputing Institute, and the vpp800/13 supercomputer system of the Institute for Space and Astronautical Science (Japan).

---

[1] H.G. Bungenberg de Jong, *Colloid Science*, vol.2, edited by H.R. Kruyt (Elsevier, 1949) 259-330.  
 [2] E.Gonzales-Tovar, M.Lozada-Cassou, and D.J. Henderson, *J. Chem.Phys.* 83, 361 (1985).  
 [3] H.Greberg, and R.Kjellander, *J.Chem.Phys.* 108, 2940 (1998).  
 [4] T.T.Nguyen, A.Yu. Grosberg and B.I. Shklovskii, *Phys. Rev. Lett.* 85, 1568 (2000).  
 [5] R.Messina, C.Holm and K.Kremer, *Phys. Rev.Lett.* 85, 872 (2000).  
 [6] M.Tanaka and A.Yu. Grosberg, *J.Chem.Phys.* 115, 567 (2001).

- [7] M.Tanaka and A.Yu. Grosberg, *Euro.Phys.J., E7*, 371 (2002).
- [8] M.Lozada-Cassou, E.Gonzales-Tovar, and W.Olivares, *Phys.Rev. E* **60**, R17 (1999); M.Lozada-Cassou and E.Gonzales-Tovar, *J.Colloid Interf.Sci.* **239**, 285 (2001).
- [9] A.Yu. Grosberg, T.T. Nguyen, and B.I. Shklovskii, *Reviews Modern Phys.*, **74**, 329 (2002).
- [10] A.V.Kabanov, V.A.Kabanov, *Bioconj.Chem.*, **6**, 7 (1995).
- [11] D.Long, J.-L.Viovy, and A.Ajdari, *Phys.Rev.Lett.*, **76**, 3858 (1996).
- [12] M.Tanaka and A.Yu. Grosberg, *Bull.Amer.Phys.Soc.* **48**, 1233 (2003).
- [13] A.Z.Panagiotopoulos and M.E.Fisher, *Phys.Rev.Lett.* **88**, 045701 (2002).
- [14] T.T.Nguyen and B.I. Shklovskii, *Phys.Rev.Lett.*, 018101 (2002).